water

MDPI

Article

Sustainable Development of Coastal Areas: Port Expansion with Small Impacts on Estuarine Hydrodynamics and Sediment Transport Pattern

Pablo Dias da Silva [1,*], Elisa Helena Fernandes [1] and Glauber Acunha Gonçalves [2]

[1] Laboratório de Oceanografia Costeira e Estuarina, Instituto de Oceanografia, Universidade Federal do Rio Grande (FURG), CP 474, Rio Grande 96201-900, Brazil
[2] Centro de Ciências Computacionais, Universidade Federal do Rio Grande (FURG), CP 474, Rio Grande 96201-900, Brazil
* Correspondence: pdsilva5@gmail.com

Abstract: With the expansion of global trade and the growing traffic of increasingly larger ships to meet this demand, the need to expand port infrastructure appears as the main alternative. In this way, dredging operations for the maintenance and deepening of navigation channels, as well as the expansion of evolution basins and berthing wharf areas become fundamental, generating large amounts of material removed from the bottom. Aiming at port expansion based on a sustainable development and minimization of the environmental impacts generated by these operations, it is necessary to seek alternatives for the destination of large volumes of dredged material. A sustainable alternative is to dispose these volumes on land in order to expand coastal areas (such as fattening beaches) and mooring pier areas. The present work presents a numerical modeling case study using the TELEMAC-3D model coupled to the suspended sediment module SEDI-3D. As an alternative, an existing island (Ilha do Terrapleno) will receive material dredged from the access channel to the Port of Rio Grande (southern Brazil) and will have its mooring area expanded. The study evaluated the impact that this change in the island's configuration would generate on the hydrodynamics and on the deposition patterns of fine suspended sediments in its surroundings and in the adjacent navigation channel. Results indicated that in the navigation channel adjacent to Ilha do Terrapleno, the new configuration promoted changes in the hydrodynamics with a decrease in the mean current velocity around the island and throughout the water column, mainly in the north and central portions of the channel. This difference decreased towards the southern portion of the channel. This change in local hydrodynamics promoted small changes in the suspended sediment deposition patterns and in the bottom evolution. Thus, the sustainable expansion of the Port of Rio Grande operational capacity considering the creation of 3600 m of berthing wharf areas and minimum environmental impact proved viable when considering the Ilha do Terrapleno proposed configuration. Furthermore, this idea offers the possibility to dispose in land 722,910 m^3 of dredged material, a sustainable alternative to the Port of Rio Grande development, and an inspiration for the sustainable development of other ports worldwide.

Keywords: ports expansion; estuaries; deposition; numerical modeling; TELEMAC-3D

Citation: da Silva, P.D.; Fernandes, E.H.; Gonçalves, G.A. Sustainable Development of Coastal Areas: Port Expansion with Small Impacts on Estuarine Hydrodynamics and Sediment Transport Pattern. *Water* **2022**, *14*, 3300. https://doi.org/10.3390/w14203300

Academic Editors: Heqin Cheng and Yijun Xu

Received: 30 August 2022
Accepted: 8 October 2022
Published: 19 October 2022

1. Introduction

The growing demand of global trade results in the need for expanding port infrastructure around the world [1]. In order to do that, it is necessary to carry out large dredging operations for the maintenance and deepening of navigation channels and the establishment of new evolution and mooring basins. In most cases, these port infrastructure demands are located near or within estuarine regions, and the more important ones are in the ports of Shanghai, Rotterdam, Antwerp, Hamburg, Los Angeles and New York. These regions, in addition to having a large concentration of population and relevant socio-economic activity,

are also regions of high biological diversity, serving as breeding and nursery sites for several species. Thus, it is essential to think of port expansion as a sustainable development process, with permanent concern regarding the destination of the generated large volumes of dredged material in order to minimize its environmental impacts. Usually, the destination given to this material, which has few possibilities for reuse as it is highly compressible and has low resistance, is to discharge into the water column of coastal disposal sites [2–4], at depths which have previously been shown to be safe to prevent their remobilization. This alternative has low environmental impact but high costs and presents potential risks for the surrounding ecosystem due to the virtual chemical contamination of this material and to its sedimentological characteristics [5,6].

In recent decades, several numerical models have been used to study the dynamics of suspended sediments in coastal and port regions [7–9] and to study the fate of suspended sediment plumes generated both at the dredging site and at the disposal sites [3]. These tools, associated with satellite images of high temporal and spatial resolution, contribute to the understanding of the dynamics of fine suspended sediments [10,11], so that the environmental impact of dredging operations can be better understood and minimized. In [12], the authors used the MIKE 21HD model to study the fate of the dispersion plume generated by the disposal of dredged material from the port of Karanja Creek, India, in four locations close to the coast. The ROMS model together with remote sensing products were used by [13] to study the seasonal variability of the pycnocline depth during the dispersion of the suspended sediment plume generated due to a mining operation at the Korean south coast. Also using the association of a numerical model (Delft3D) and remote sensing, [14] investigated the spatio-temporal variation of suspended sediment concentration due to sand dredging activities in Lake Poyang, China. More recently, [3] investigated the plume dispersion patterns of dredged material from the Port of Rio Grande access channel using the TELEMAC-3D numerical model and investigating four proposed dumping sites in the coastal region.

Another alternative that has been applied for dredged material is land disposal. In [15], the authors used a tool called Life Cycle Assessment (LCA) to assess the extent and impacts associated with the dredging and disposal process off the coast of the Mediterranean Sea at the Port of Damietta, Egypt. The authors demonstrated that land disposal would reduce the environmental impact by 80% compared to the disposal in the Mediterranean Sea. More recently, the land disposal practice used in shoreline fattening and expansion of port infrastructure is currently under development in the Port of Gothenburg, in Sweden. This port is currently undergoing its biggest expansion since the 1970s and will use around 180,000 m^3 of dredged material as fill for the construction of a 140,000 m^2 terminal, scheduled for completion in 2023 (https://www.portofgothenburg.com/news-room/press-releases/dredging-spoils-transform-into-new-terminal-at-the-port-of-gothenburg/ (accessed on 10 December 2021).

The reuse of dredged material, however, depends on its characteristics, and requires prior knowledge about the hydrodynamics and sedimentary dynamics of the region, with special interest in patterns of deposition and erosion of sediments, as well as predictive studies on the impact of the proposed changes in these processes [16]. Furthermore, this strategy can have impacts on the surroundings of port regions, both in terms of socio-economic viability in highly urbanized regions, and in environmental aspects, as these estuarine regions have sensitive ecosystems [17–19]. Thus, this sustainable development alternative must be extensively investigated prior to any real environmental alteration.

Studies using numerical modeling techniques have been carried out to investigate deposition and erosion patterns in response to port expansion alternatives. In the Port of Figueiras, Spain, [20] the authors used numerical modeling techniques (Delft3D) to assess the effects of the port expansion on the estuarine activity considering twelve scenarios before and after port the engineering work. In [16], the author achieved effective results for the use of dredged material (sand) from port channels to help minimize coastal erosion in strategic regions near the Nile Delta using the Delft3D model. His results demonstrated

that the direct use of dredged materials is a viable alternative, avoiding possible negative impacts due to the construction of rigid structures. More recently, [21], used the MIKE 21 model to estimate bathymetric changes and the alteration of sedimentation rates due to the expansion of a breakwater in the Port of Nowshar, Iran. All these studies suggest the importance of using numerical modeling techniques to contribute for the sustainable development of port regions by assessing the environmental impacts produced by the expansion of port capacity around the world prior to any real modification.

In [22], the authors used the TELEMAC-3D hydrodynamic model coupled with the SediMorph morphodynamic module to study changes in the deposition patterns of fine suspended sediment after the expansion of two marine structures (jetties) that protect the access channel to the Port of Rio Grande, Brazil. The authors observed an increase in the deposition pattern in the port access channel and the redirection of the ebb flow jet at the mouth of the estuary, resulting in a change in the coastal suspended sediment distribution pattern and alteration of the final destination of this material in the coastal zone when compared to the old structure. In the same region, in the last two dredging operations (2013 and 2019–2020), the Port of Rio Grande Authority (PORTOS RS) used a site located in the coastal region as a dump site for the dredged material, according to the environmental licensing granted by the Brazilian Environmental Institute and Renewable Natural Resources (IBAMA). This dump site is 6 × 6 km and is located at approximately 20 km off the coast at a depth of 21 m. On these occasions, approximately 1,600,000 and 18,000,000 m^3 of dredged material, respectively, mainly composed of clay and silt, were disposed of at this dump site. Thus, the recent increase in the frequency and volume dredged in the Port of Rio Grande brings to discussion the establishment of sustainable alternatives for the destination of the dredged material.

More recently [3], presented a comparison between four scenarios for the ocean disposal of dredged material from the Port of Rio Grande access channel based on numerical modeling experiments (TELEMAC-3D). The study presents a comparison between the tendency of the dispersion plume generated by the discharge of 3,000,000 m^3 of material to return to the shoreline (or not). Modeling results showed that in the investigated sites closer to the shoreline the dumped material remained in place, while in the sites located in deeper areas the dumped material tends to spread alongshore in accordance with the predominant wind directions (NE–SW). Furthermore, the model estimated for all the investigated sites that 96 h after the end of the discharge, the suspended sediment concentration returns to its usual value for the region (~0.05 g/L). Considering the quantities, frequency of dumping and the usual suspended sediment concentration values for the region, the authors concluded that the actual licensed dumping site presents the smaller environmental impact. The idea to dispose this dredged material inland and expand the port structure in a more sustainable way, however, was not evaluated.

Thus, the present work presents a study to evaluate potential hydrodynamic changes and consequent alterations in the transport and deposition patterns of suspended sediments in the channel adjacent to Ilha do Terrapleno, located in the inner area of the Port of Rio Grande (Figure 1), when considering a sustainable port expansion scenario proposed by the Port of Rio Grande Authority.

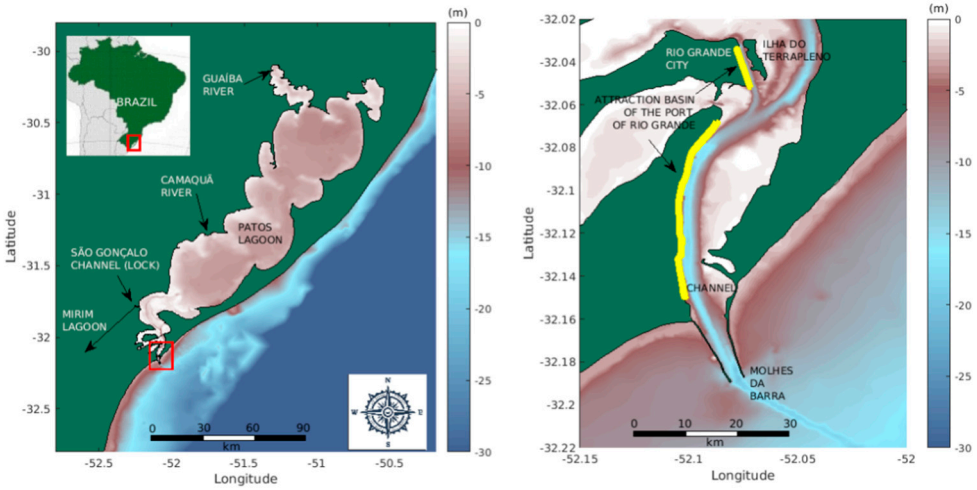

Figure 1. Left panel—Patos Lagoon and its main tributaries. **Right** panel—Zoomed-in view of the lower Patos Lagoon estuary, showing the position of Ilha do Terrapleno and the mooring terminals of the Port of Rio Grande (yellow area). Figure uses actual bathymetric data provided by the Brazilian Navy and Rio Grande Port Authority and interpolated for the domain.

2. Study Area

Patos Lagoon, located in southern Brazil (30°–32° S latitude and 50°–52° W longitude) (Figure 1), is the largest choked coastal lagoon in the world [23], and is connected to the South Atlantic Ocean through a narrow channel (<700 m wide), which intermittently exports fine suspended sediment to the coastal region due to the continental discharge and wind effects [24–27]. The region is under the influence of microtides, with 0.3 m of mean amplitude [28].

The main supply of freshwater and fine suspended sediment to the lagoon comes from two rivers located in the north and central regions of the lagoon, Guaíba River and Camaquã River (Figure 1), respectively, which drain a basin of approximately 200,000 km^2. The average water discharge of these rivers is 1770 m^3 s^{-1} [29], but as they are located in a subtropical mid-latitude region their hydrology presents a seasonal variation, [27]. A third source of continental waters and fine suspended sediments to the lagoon is the São Gonçalo Channel, which connects the Patos Lagoon to the Mirim Lagoon. Interannual variations in these freshwater continental contributions were observed and related to ENSO events [11], with the freshwater discharge into the lagoon exceeding 13,000 m^3 s^{-1} in El Niño years [30]. In [31], the authors also identified interdecadal variability in these freshwater contributions.

During periods of low discharge (<2000 m^3 s^{-1}) the Patos Lagoon dynamics is controlled by the combination between the freshwater discharge of the main tributaries and the remote and local effects of the wind (Möller and Castaing, 1999). During Southwest (Northeast) wind events, the remote wind effect promotes an increase (decrease) in the water level at the coast, resulting in a flood (ebb) regime in the lagoon. During periods of high discharge (>2000 m^3 s^{-1}), the continental freshwater contribution dominates the dynamics of the lagoon.

The Port of Rio Grande (http://www.portoriogrande.com.br (accessed on 10 December 2021), located inside the Patos Lagoon estuary (Figure 1), is currently one of the most important ports in Brazil. In recent decades, its navigation channels have faced an aggravation of siltation, generating the need to carry out dredging of greater volumes and in higher frequency. According to [32], this aggravation of siltation is related to an increase in the supply of suspended sediment associated with an increase in precipitation in its basin due to ENSO events. Another important factor is unsustainable farming, which promotes the erosion of the Patos Lagoon margins.

Recently, the increase in the frequency and volume dredged brought to discussion alternatives for the destination of the dredged material previously discarded at the coastal

disposal site, and a land disposal site at Ilha do Terrapleno (Figure 1) was considered by the Port of Rio Grande Authority as an alternative for sustainable port expansion. Its environmental impacts, however, needed to be addressed before execution of the work to confirm this as a viable sustainable alternative for dredged material disposal. The idea was to change the Ilha do Terrapleno geomorphology in order to maximize landfill and establish an extra mooring pier in a region where the access channel has 11 m of depth.

3. Methods

3.1. Numerical Model

The hydrodynamic model TELEMAC-3D (http://www.opentelemac.org (accessed on 5 December 2020), version V7P0, coupled to its suspended sediment module SED-3D, was used to investigate changes in the hydrodynamics and suspended sediment deposition patterns around Ilha do Terrapleno based on the actual and proposed configurations (Figure 2). TELEMAC-3D solves the Reynolds-averaged Navier–Stokes equations assuming (this study) or not the hydrostatic pressure condition and considering the Boussinesq approximation [33]. For this study, the vertical turbulence model of Mixing length and the Smagorinsky model for horizontal turbulence were used (Table 1). The model considers the evolution of the free surface as a function of time and uses advection-diffusion equations to transport tracer concentrations such as salinity, suspended sediment and temperature (Equation (1)). The suspended sediment concentration is resolved by the SED-3D module, where its characteristics are specified (Table 2). The module considers the flocculation process based on the [34] formula and the deposition and resuspension rates based on the [35] formula. The main results obtained at each point of the computational grid are the flow velocity in the three directions and the concentration of the transported quantities, and the free surface elevation at the surface.

$$\frac{\partial C}{\partial t} + u\frac{\partial C}{\partial x} + v\frac{\partial C}{\partial y} + w\frac{\partial C}{\partial z} + \frac{\partial (W_c C)}{\partial z} = \frac{\partial}{x}\left(K_x \frac{\partial C}{\partial x}\right) + \frac{\partial}{y}\left(K_y \frac{\partial C}{\partial y}\right) + \frac{\partial}{z}\left(K_z \frac{\partial C}{\partial z}\right) \quad (1)$$

where u, v and w represent flow velocities (m s^{-1}); C is the concentration of suspended sediment (kg m^{-3}); W_c is suspended sediment settling velocity (m^2 s^{-1}); K_x, K_y and K_z are coefficients of turbulent sediment diffusion (m^2 s^{-1}).

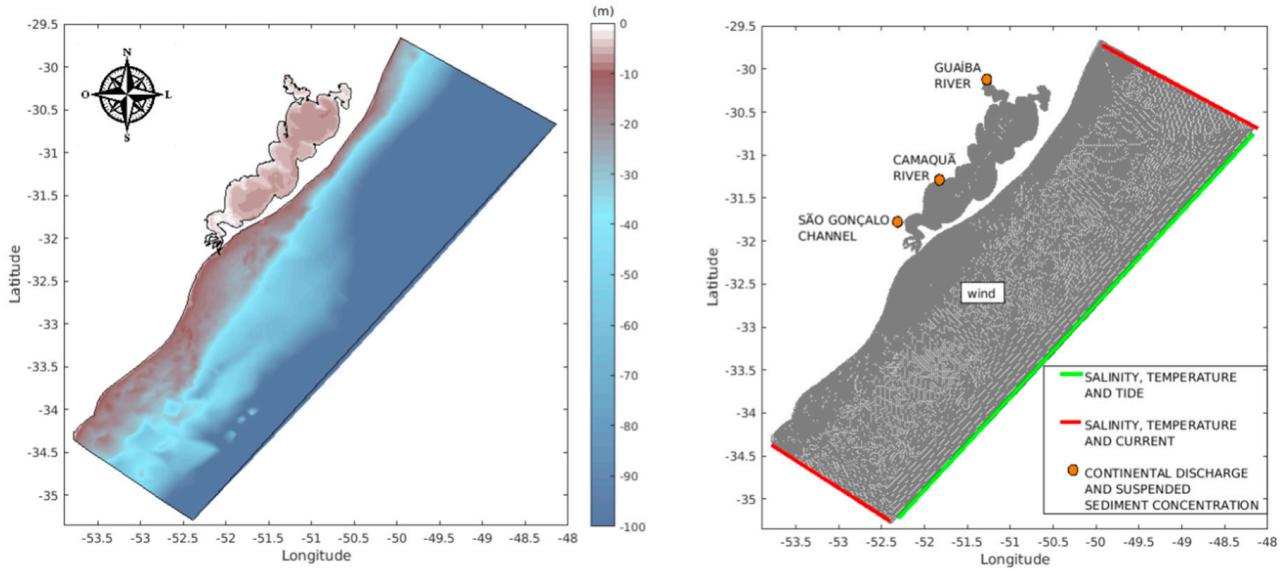

Figure 2. *Cont.*

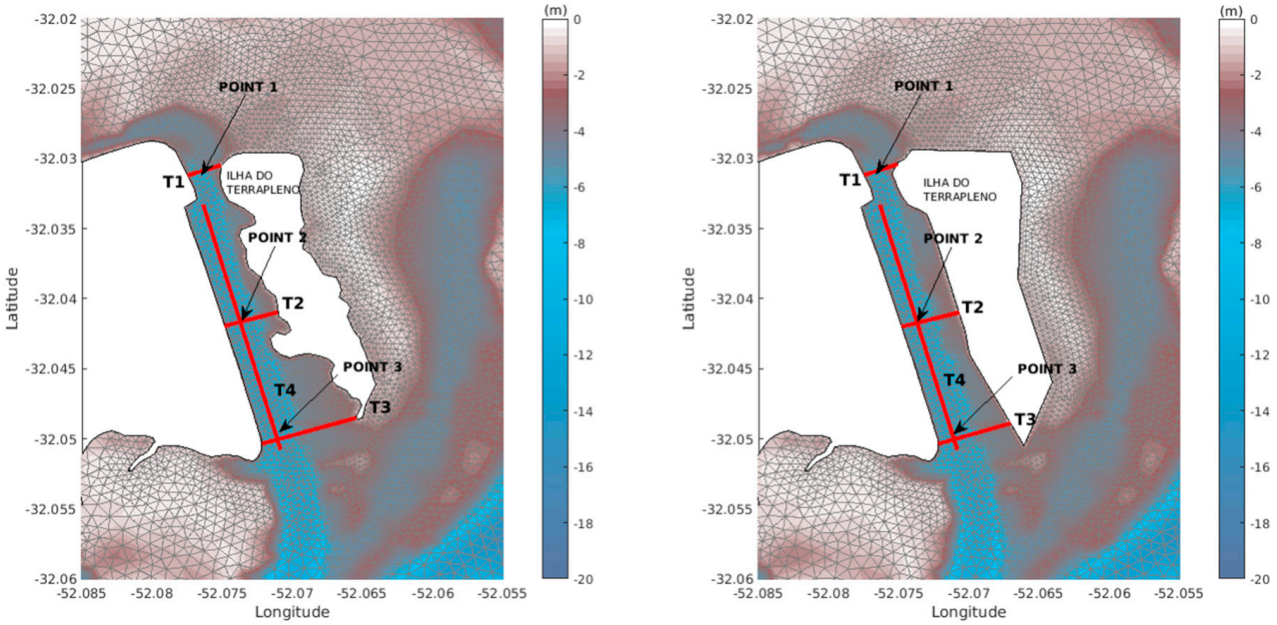

Figure 2. Top panel—Model domain with bathymetric information in the color scale and the numerical grid identifying the open boundaries and applied boundary conditions for both simulations. **Bottom** panel—Zoom-in view of the numerical grid with the actual and proposed morphology for Ilha do Terrapleno. Red transects and points indicate areas from where results were extracted for analysis.

Table 1. The best set of physical parameters resulting from the calibration exercise of the TELEMAC-3D model.

Parameter	Value
Time step	90 s
Coriolis coefficient	-7.70735×10^{-5}
Horizontal turbulence model	Smagorinski
Vertical turbulence model	Mixing length
Mixing length scale	10 m
Tidal flats	Yes
Law of bottom friction	Nikuradse
Coefficient of wind influence	5×10^{-6} N·m^{-1}·s^{-1}

Table 2. Parameters for the suspended sediment SED-3D module.

Parameter	Value
Suspended sediment class	Fine silt
Mean diameter of the sediment	1×10^{-5} m
Critical shear stress for erosion	1.5 N·m^{-2}
Critical shear stress for deposition	0.01 N·m^{-2}
Cohesive sediment	Yes
Density of the sediment	2650 kg·m^{-3}
Flocculation formula	Van Leussen
Sediment settling velocity	0.00001 m·s^{-1}

3.2. Numerical Grid and Initial and Boundary Conditions

The computational domain of this study covers the region between 29.5°–35.5° S and 48°–54° W (Figure 2), and the bathymetric data used were digitized from nautical charts of the Brazilian Navy and complemented with data provided by the Port of Rio Grande Authority. The domain for these simulations considers the Patos Lagoon and extends to a

depth of 2300 m in the oceanic contour so that larger scale model outputs can be used as boundary conditions for the simulations.

The domain was discretized into unstructured computational grids that use triangular finite elements of variable size (Figure 2), using the BlueKenue Software (http://www.nrc-cnrc.gc.ca/eng/solutions/advisory/blue_kenue_index.html (accessed on 10 October 2019). This technique allows better refinement in regions with large bathymetric gradients and complex morphology, and less refinement in regions of less interest. The grid generated for the simulation with the current configuration of Ilha do Terrapleno is composed of 52,098 points, while the grid with the proposed configuration is composed of 51,790 points (Figure 2). Two identical simulations were carried out for a two-year period, from 1 January 2013 to 31 December 2014 and in both simulations, vertical discretization was performed with 7 Sigma levels.

Initial salinity and temperature fields were prescribed based on the results of the HYCOM + NCODA Global Project (HYbrid Coordinate Ocean Model, https://hycom.org/ (accessed on 5 December 2019), which have temporal resolution of 1 day and spatial resolution of $0.083^\circ \times 0.083^\circ$. Initial suspended sediment concentrations were considered null throughout the domain. The open boundaries in the computational grid were divided into continental, oceanic and surface boundaries, where different boundary conditions were prescribed (Figure 2) to carry out the simulations. The remaining contours were considered closed.

At the oceanic borders, the OSU Tidal Inversion System (OTIS [36]) was used to prescribe the water level, providing the sea surface elevation and the regional tidal flow velocity. The water level was calculated by the inverse solution of the Laplace equations for the tide, using data collected by the TOPEX/POSEIDON Project (http://volkov.oce.orst.edu/tides/global.html (accessed on 6 December 2019), which was made available internally in the TELEMAC-3D Model. Thus, 33 harmonic tidal components were considered a reliable estimate of the ocean surface variation. Once the sea level rise was known at an edge point, the Continuity Equation was integrated, and the flow velocity components were obtained.

The surface boundary of the computational grid was dynamically forced with wind intensity and direction results from the ECMWF global model (European Center for Medium-Range Weather Forecast, http://www.ecmwf.int/ (accessed on 7 December 2019), with a temporal resolution of 24 h and a spatial resolution of 0.75°, being these results interpolated for each grid point. For the continental boundaries, daily continental freshwater discharge data from Guaíba River and Camaquã River obtained from the National Water Agency (ANA, http://www.ana.gov.br (accessed on 8 December 2019) were prescribed. For the São Gonçalo Channel, water level data obtained from the Mirim Lagoon Agency (ALM, https://wp.ufpel.edu.br/alm/agencia (accessed on 8 December 2019) were used and transformed into daily discharge data using a rating curve method proposed by [37], and then calculated its climatology for the time interval 1991–2012. One class of suspended sediment was used in this study, fine silt, with an average diameter of 1×10^{-5} m. The concentrations of fine suspended sediment prescribed at the continental boundaries were 0.35 kg m^{-3}, 0.2 kg m^{-3} and 0.25 kg m^{-3} for Guaíba River, Camaquã River and São Gonçalo Channel, respectively. Values of the same order were used in previous studies by [3,7]

3.3. Calibration and Validation

The ability of the numerical model to reproduce the environmental conditions was evaluated by comparing the model results and measured time series of flow velocity and salinity for the same period and calculating the RMAE (Relative Mean Absolute Error) and the RMSE (Root Mean Square Error) parameters. The RMAE allows classifying the quality of results on a scale from bad to excellent [38], while the RMSE reports the magnitude of the error with dimensional values.

The calibration for the TELEMAC-3D hydrodynamic model was carried out for December 2011. The current velocity data were obtained by an Acoustic Doppler Profiler, with temporal resolution of 1 h, anchored at Praticagem Station at 12 m depth (Figure 3A). This

equipment has a maximum profiling range (m) of 25–30 m, covering a range of ±10 m s^{-1}, with a resolution of 0.1 cm s^{-1} and accuracy: ±1% of measured velocity, ±0.5 cm s^{-1}. For the validation of the hydrodynamic model, salinity data from January 2017 obtained by a SBE CT 37SM (Conductivity and Temperature), anchored at 4 m depth (Figure 3A) with an hourly acquisition rate were used. This equipment has a measurement range of conductivity: 0 to 7 S m^{-1} (0 to 70 mS cm^{-1}), resolution conductivity: 0.00001 S.m^{-1} (0.0001 mS cm^{-1}) and initial accuracy conductivity: ± 0.0003 S m^{-1} (0.003 mS cm^{-1}). The model was run using the same type of initial and boundary conditions presented in Section 3.2, but for the selected calibration and validation periods.

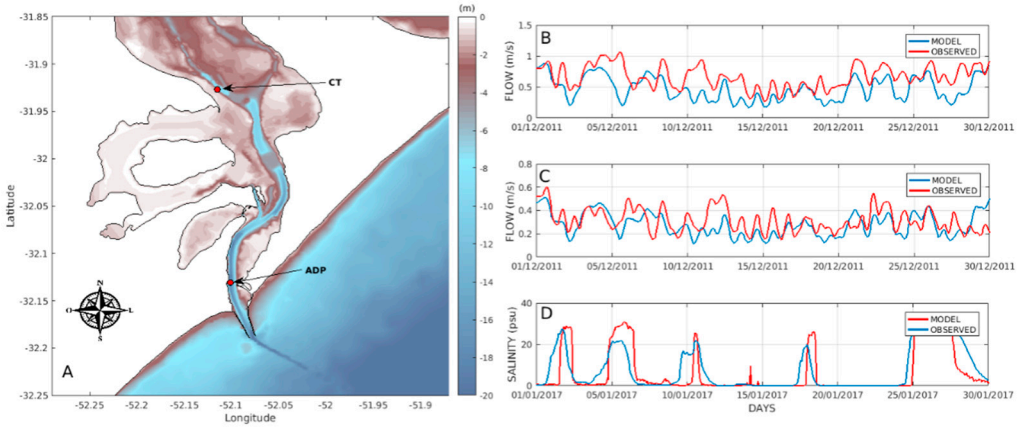

Figure 3. (**A**) Location of stations from where measured data were obtained in December 2011 and January 2017. Current velocity at the surface (**B**) and at 12 m (**C**) during the calibration exercise and salinity at 4 m (**D**) during the validation of the hydrodynamic model.

Figure 3B,C indicate that the model does represent well the trends of increase and decrease in current velocity. The calculated RMAE was 0.29 at the surface and 0.13 at 12 m depth, classifying the model's reproduction as good and excellent, respectively, according to [38] (Table 3). The calculated RMSE was 0.26 m s^{-1} at the surface and 0.11 m s^{-1} at 12 m. Figure 3D shows measured and calculated time series of salinity at a depth of 4 m. The calculated RMSE was 7.37 psu (within a range from 0 to 35) and the RMAE was 0.23, which classifies the model's reproduction as good.

Table 3. Model reproduction classification based on the RMAE [38].

Qualification	Excellent	Good	Reasonable/Fair	Poor	Bad
RMAE	<0.2	0.2–0.4	0.4–0.7	0.7–1.0	>1.0

The parameters used in the calibration and validation of the suspended sediment module were presented by [32] and summarized in Table 2 for this numerical grid.

Although the model satisfactorily reproduces the measured variables based on the chosen methodology [38], it is important to point out that some approximations were inevitable in the set-up of the simulations. Due to the lack of freshwater discharge time series for the São Gonçalo Channel during the simulated period, this open boundary was forced with a freshwater discharge climatology (from 1991–2012). According to the study carried out by [39], this kind of approximation is expected to generate an underestimation of the freshwater contribution from Mirim Lagoon and consequently affecting the model calibration and validation. Another important aspect is that the São Gonçalo channel has a lock that is kept closed to prevent salinity from Patos Lagoon to reach Mirim Lagoon (Figure 1). Thus, this anthropogenic impact on the natural salinization of both systems is poorly represented in the hydrodynamic model, affecting the natural dilution of coastal waters inside Patos Lagoon estuary and the model predictions. These and other observations are reported by [40] when applying water quality models.

The model also has some limitations in the parametrization of important processes such as the turbulent processes of diffusion and dispersion. This limitation is a reality in most numerical models and particularly for the present study, can impact the model´s predictions around areas of complex morphology and especially around islands. Studies presented by [41,42] report the effect that submerged vegetated regions promote on flows and sediment transport, which are generally poorly represented in models. Such expected impacts will also affect numerical model predictions of sediment transport. Although we are aware of these inevitable approximations in the numerical model, and they must be kept in mind when analyzing the results, we are confident about the quality of the model predictions, especially because the study was based on a comparative analysis between two scenarios.

4. Results

4.1. Flow Velocity and Suspended Sediment Concentration at the Mouth

Figure 4 present estimated values for the flow velocity calculated at the mouth of the jetties (Figure 1) for the entire simulation period (1 January 2013–31 December 2014). The average water discharge was estimated as 2196 m^3 s^{-1}, and the suspended sediment transport exported to the coastal zone in the same period was 1.02 × 10^4 t day^{-1} for both simulations (actual and proposed Ilha do Terrapleno configuration).

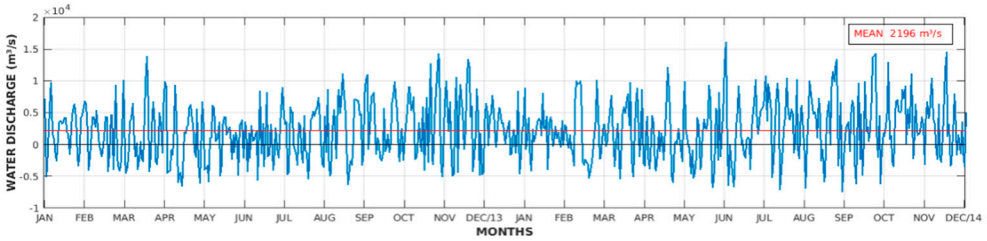

Figure 4. Water discharge at the mouth of the jetties calculated by the model for the simulation period for both simulated scenarios. Red line represents the mean value.

4.2. Comparative Hydrodynamics between Simulated Scenarios

Time series of calculated depth-averaged current velocities were extracted at points P1, P2 and P3 (Figure 2), to draw a comparison between the two scenarios and assess the changes in hydrodynamics in the channel region (Figure 5). At point P1 (Figure 2), the configuration proposed for Ilha do Terrapleno generated an increase of 0.06 m/s in the mean velocity in relation to the actual configuration (Figure 5A). For point P2, the proposed configuration generated a slight decrease in the mean velocity of 0.02 m/s (Figure 5B), while for P3 no alteration in the current velocities was observed (Figure 5C).

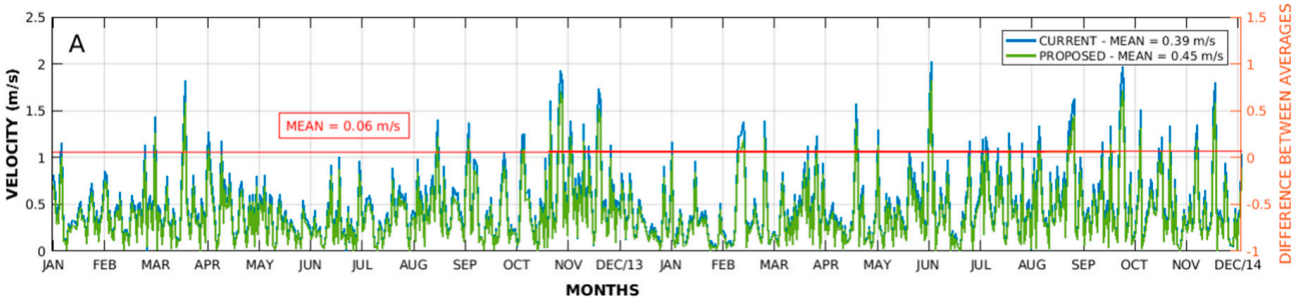

Figure 5. *Cont.*

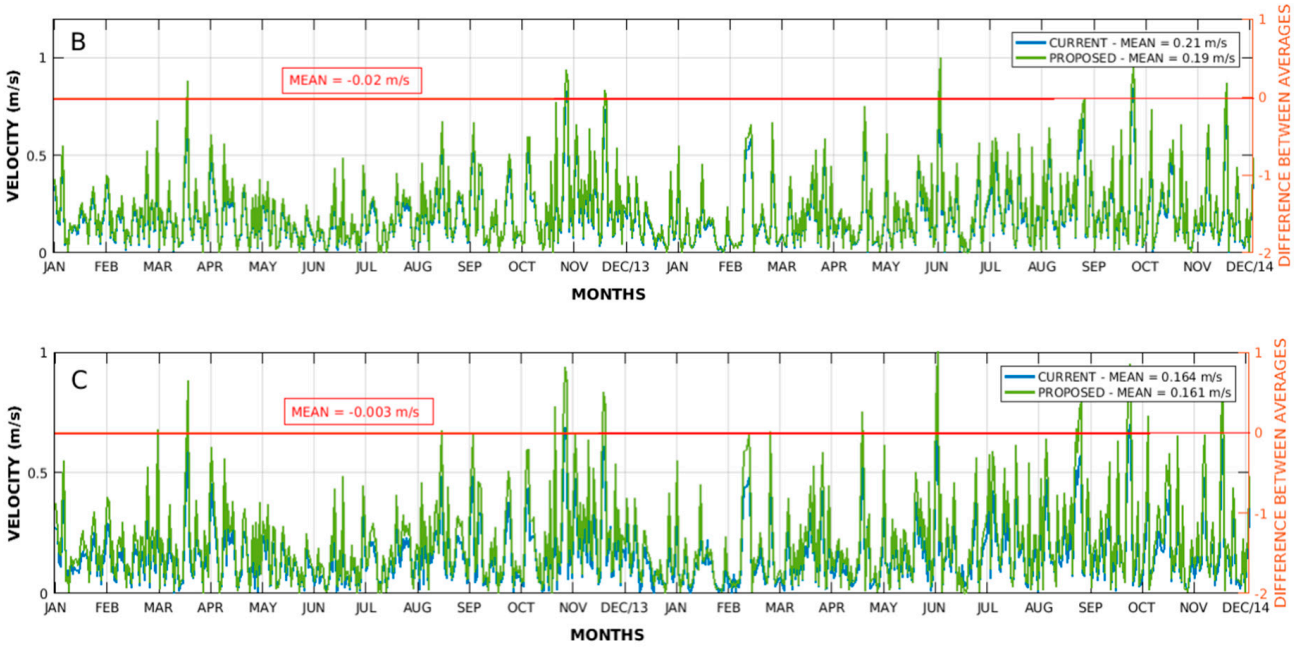

Figure 5. Left axis—Comparative hydrodynamics between simulated scenarios. Time series of the depth-averaged current velocities for both simulated scenarios at points P1 (**A**), P2 (**B**) and P3 (**C**). Right axis—Difference between depth-averaged current velocities calculated for the actual and proposed Ilha do Terrapleno scenarios. Red line represents the difference between mean current velocity for the actual and proposed scenarios.

In order to analyze potential changes in the intensity and direction of the current velocity field around Ilha do Terrapleno, Figure 6 presents the mean depth-averaged current velocities for the actual (Figure 6A) and for the proposed configuration (Figure 6B) for the island, and the difference between them (Figure 6C) for the entire simulation period. It is possible to observe a decrease in the mean depth-averaged current velocity throughout the main channel between Ilha do Terrapleno and Rio Grande city, except at the northern part of the channel.

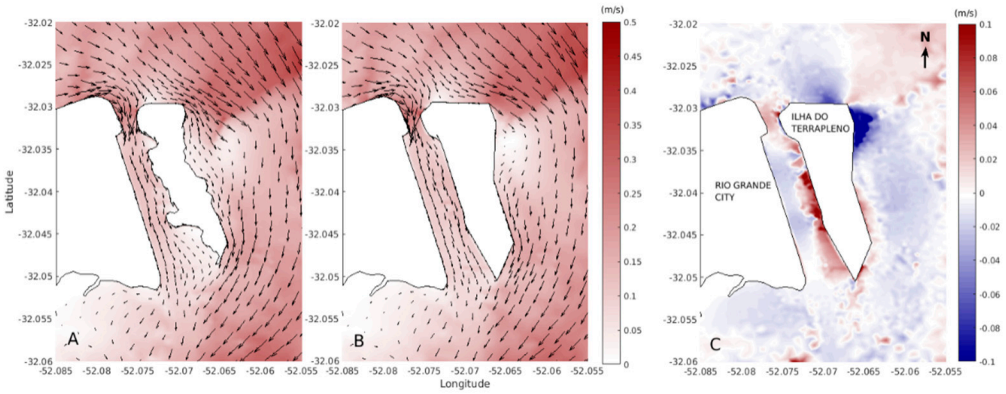

Figure 6. Calculated mean depth-averaged current velocity for the actual (**A**) and proposed (**B**) configuration for Ilha do Terrapleno and the difference between both scenarios (**C**) for the entire simulation. The color scale indicates current velocity intensity and vectors indicate current velocity direction. For the differences, positive (negative) values indicate an increase (decrease) in the mean depth-averaged current velocity. The difference is calculated by subtracting the mean depth-averaged current velocity for the proposed from the actual scenario.

Around the Ilha do Terrapleno margins, however, there is an increase in the mean depth-averaged current velocity throughout the west margin, which can reach up to

0.1 m s^{-1}. On the east margin of the island, a reduction in the mean depth-averaged current velocity of up to 0.1 m s^{-1} is observed in the north-northeast sector while a small increase in the south sector occurs.

For a better understanding of the current velocity distribution along the depth, vertical profiles of the calculated mean current velocity for points P1, P2 and P3 (Figure 2) for both scenarios are presented in Figure 7. At P1 the mean current velocity along the entire water column increased for the proposed scenario (Figure 7A). For the other points, P2 (Figure 7B) and P3 (Figure 7C), velocities are lower at the bottom and increase towards the surface in the proposed scenario for Ilha do Terrapleno.

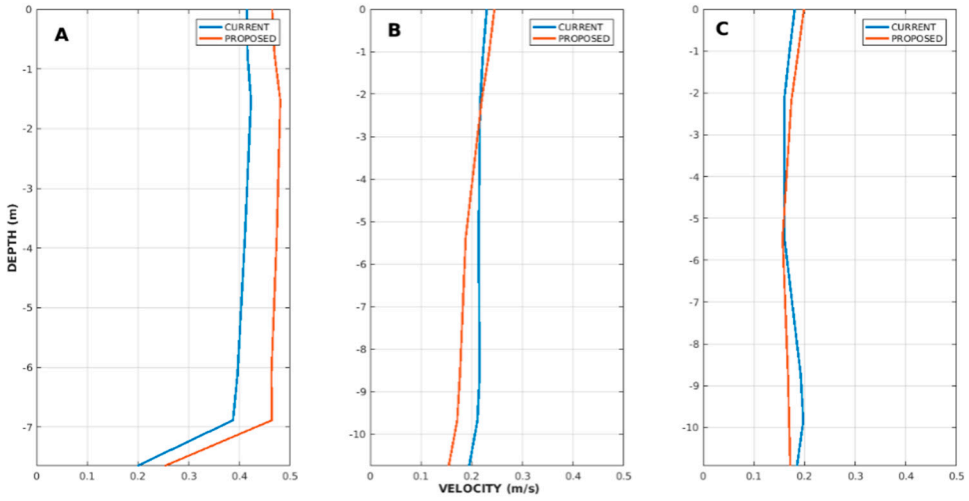

Figure 7. Mean calculated current velocity profiles for points P1 (**A**), P2 (**B**) and P3 (**C**) for both the actual and proposed scenarios for Ilha do Terrapleno.

When looking at the calculated mean current velocity at a vertical profile (T4, Figure 2) throughout the channel between Ilha do Terrapleno and the Rio Grande city for both the actual and the proposed scenarios for Ilha do Terrapleno (Figure 8), interesting results come out. Results show that the calculated mean current velocity intensity is reduced throughout the entire water column from the north to the central part of the channel, while an increase (decrease) in current velocity occurs towards the surface (bottom) in the southern part of the channel.

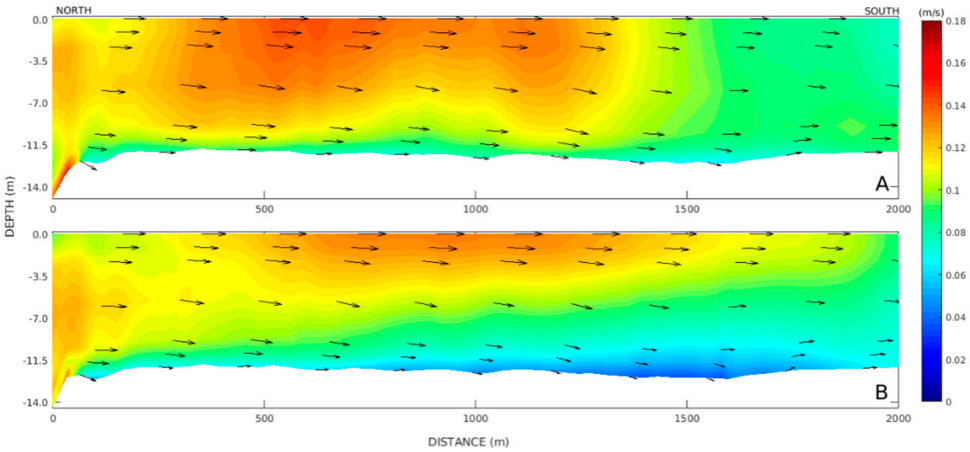

Figure 8. Calculated mean current velocity for the actual (**A**) and proposed (**B**) scenario for the entire period of simulation. The color scale indicates the current velocity intensity, and vectors indicate the direction. At the right (left) of the transect we have the north (south) end of the channel.

In order to better understand the mean current velocity behavior across the channel between Ilha do Terrapleno and Rio Grande city, results were analyzed in three transects

located in the northern (T1), central (T2) and southern (T3) parts of the channel (Figure 2), for both the actual and the proposed scenarios for Ilha do Terrapleno (Figure 9).

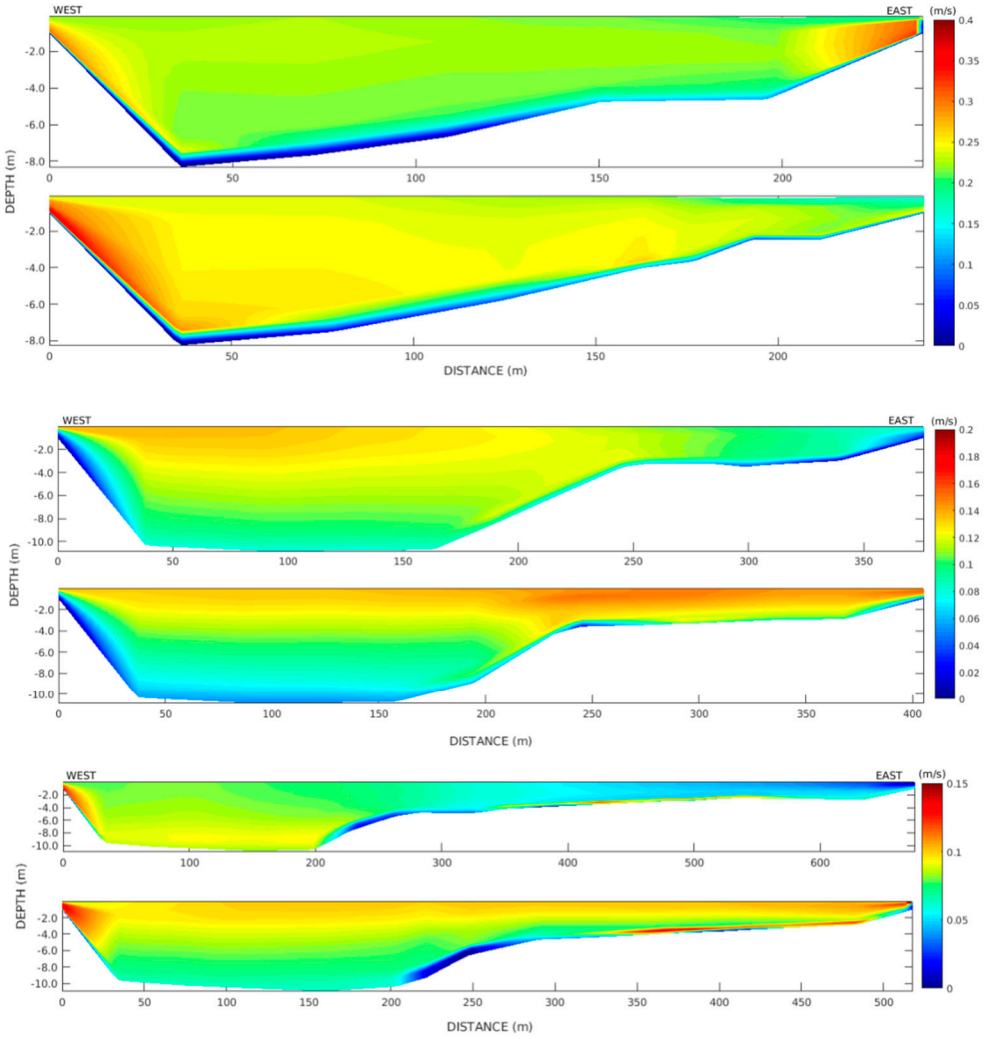

Figure 9. Mean current velocity across the channel between Ilha do Terrapleno and Rio Grande city, for both the actual (first figure) and the proposed (second figure) scenarios for Ilha do Terrapleno analyzed in three transects located in the northern (T1, **top** panel), central (T2, **central** panel) and southern (T3, **bottom** panel). West (east) limit of the transect is close to Rio Grande City (Ilha do Terrapleno).

Results indicate that at the northern part of the channel (Figure 9, T1, top panel), the proposed scenario for Ilha do Terrapleno promoted an increase (+14%) in current velocity along the transect, the only exception being the east limit (−45%) (close to Ilha do Terrapleno). In the central part of the channel (Figure 9, T2, central panel), an increase (+5%) in the current velocity occurred close to the surface and a decrease (−23%) in the deeper part of the channel when considering the proposed scenario for Ilha do Terrapleno. A similar behavior occurred at the southern part of the channel, +11% (surface) and −17% (deeper part) (Figure 9, T3, bottom panel).

4.3. Deposition of Suspended Sediment

Figure 10 presents the mean deposition flux for the actual (Figure 10A) and proposed (Figure 10B) scenarios for Ilha do Terrapleno, for the entire simulation period and the difference between them (Figure 10C). In Figure 10C, it is possible to see the tendency of an increase in the deposition flux (positive values), mainly in the central (+25%) and southern

half (+40%) of the navigation channel adjacent to Ilha do Terrapleno, and a slight decrease (negative values) in the northernmost region of the channel (−11%). Close to the west (northeast) margins of the Island, the deposition flux presents lower (higher) values, as would be expected due to the change in morphology and local hydrodynamics. This result responds to the changes in the calculated mean velocity fields (Figure 6).

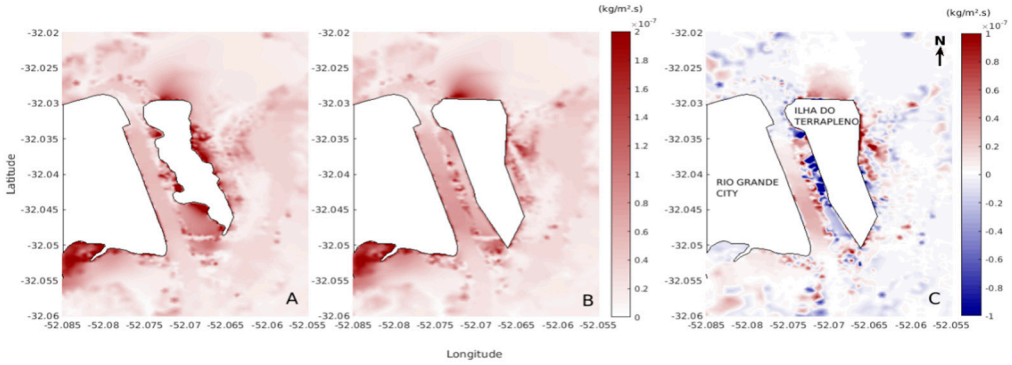

Figure 10. Average deposition flux for the (**A**) actual scenario, (**B**) proposed scenario and (**C**) difference between them. Negative (positive) values represent decrease (increase) values of deposition flux.

In order to put the mean deposition flux results in the right perspective, Figure 11 shows the bed evolution for the last day of the simulation for the two simulated scenarios and the difference between them. This parameter estimates the thickness of the layer of deposited material arising from the transport in suspension. The model estimated maximum values of bed evolution reaching up to +15 cm in each scenario (Figure 11A,B). In a comparison between scenarios (Figure 11C), positive (negative) values indicate an increase (decrease) in the deposition of material at the bottom for the proposed configuration for Ilha do Terrapleno.

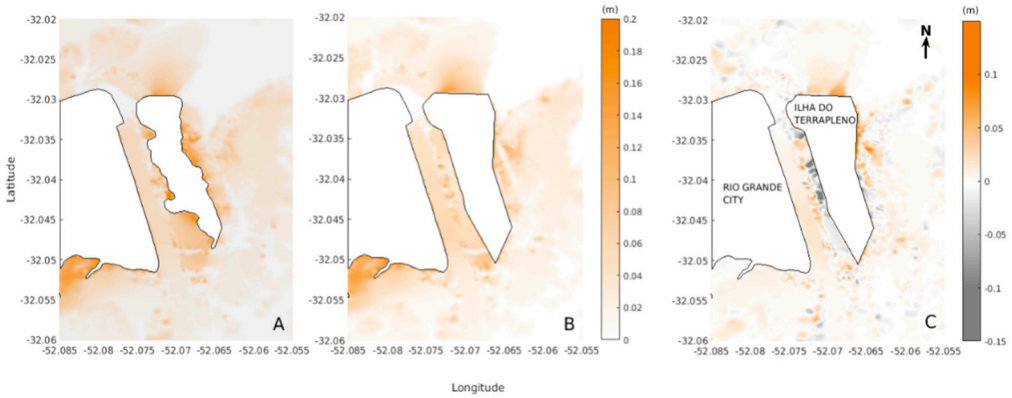

Figure 11. Bed evolution for the (**A**) actual and the (**B**) proposed scenario for Ilha do Terrapleno and (**C**) the difference between them. The difference is calculated by subtracting the bed evolution for the proposed from the actual scenario.

In Figure 11C it is possible to see a tendency of decreasing sediment deposition (negative values) in the northern portion of the navigation channel (-10%, 0.3 cm) and an increase (positive values) along the channel towards the south (+30%, 1 cm) after two years of simulation. Maximum values between −15 and 15 cm were estimated for the difference between the scenarios. Close to the margins of the island, in the North and Northeast regions, it is possible to see an increase in deposition (+31%, 2.5 cm). On the west side of the island, there is a trend of decreasing deposition (−80%, 13 cm).

In order to follow the bed evolution throughout time, time series of bed evolution for the two scenarios were extracted at Points P1, P2 and P3 (Figure 2) and are presented in Figure 12. Results indicate an increase in deposition at Points P2 (max 1 cm) and P3

(max 1 cm) (Figure 12B,C) and a decrease at point P1 (−80%, <0.1 cm), located near the North of the channel (Figure 12A). Thus, the proposed configuration for Ilha do Terrapleno presents bottom evolution values up to 25 to 30% higher for points P2 and P3 at the end of the simulation, but these percentages represent a maximum increase in bed evolution of 1 cm after two years. For Point P1, the deposition is smaller throughout the simulation, also presenting periods of resuspension, and the bottom evolution does not differ from the values for the actual configuration of Ilha do Terrapleno.

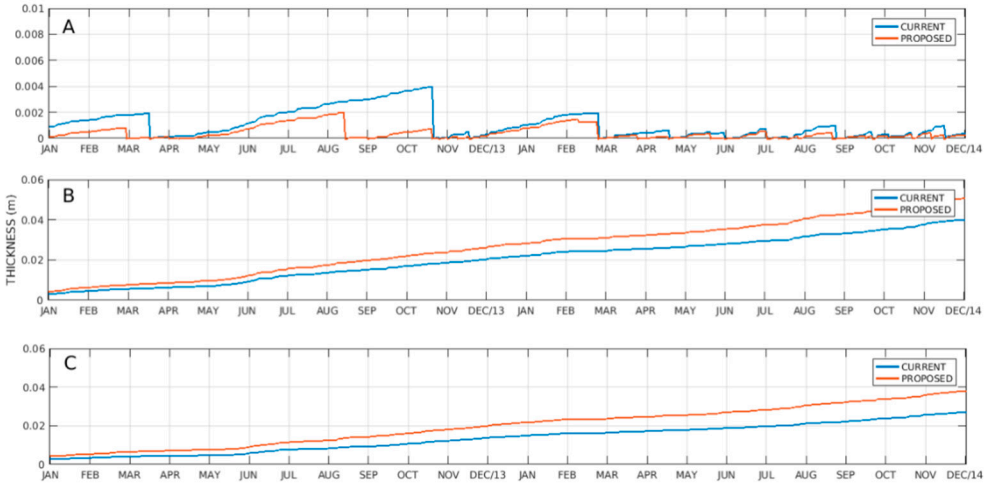

Figure 12. Bed evolution calculated for point P1 (**A**), P2 (**B**) and P3 (**C**) for both actual and proposed scenarios for Ilha do Terrapleno. The vertical scale is different to improve visualization.

5. Discussion

When analyzing the model's performance, the TELEMAC-3D hydrodynamic model showed good agreement with the data collected in situ during the calibration and validation exercises (Figure 3), reaching values of RMAE and RMSE similar to previous studies [3,7,27,43] and considered at least a good reproduction of reality. Furthermore, the SED-3D suspended sediment module was set-up with the parameterization previously applied on studies of the Patos Lagoon suspended sediment dynamics [3,7,32], where a good agreement with in situ and satellite data was obtained [7,32]. Thus, the authors are confident that both modules are adequate tools for the proposed study.

This numerical modeling tool was then applied to evaluate changes in the hydrodynamics and suspended sediment transport patterns in the Patos Lagoon estuary due to a sustainable expansion of the Port of Rio Grande. The study case was Ilha do Terrapleno, a small island located inside the estuary, which at present is not part of the port infrastructure. Results from numerical simulations were compared for the actual and proposed scenarios for Ilha do Terrapleno (Figure 2). The proposed scenario for the island considers an enlargement of the northeast (268,384 m^2) and southwest (122,378 m^2) areas of the island and the linearization of its margins, resulting in 3600 m of new berthing wharf areas (Figure 13). These new areas around the island (white areas, Figure 13) represent the opportunity to disposal 722,910 m^3 of dredged material in-land, an excellent sustainable port development exercise. This volume was calculated to fill the areas up to the estuary water reduction level. Then, from this level, an elevation of 1 m was considered to align with the average level of the topography of the edge of the island. Depending on the type of soil to be used in the landfill and on its granulometric characteristic and compaction rates, however, the required volume can change.

Constructions and alterations of port and maritime infrastructures inevitably affect the dynamics of their surroundings and must be carried out aiming at the best cost–benefit, both in economic and environmental terms [44]. Results of the present study for the actual and proposed scenarios for Ilha do Terrapleno (Figure 2) were analyzed in terms of export of fine suspended sediment, mean current velocity fields and deposition patterns of fine

suspended sediment around the island. Particularly for the export of fine suspended sediment towards the coast, this study calculated 1.02×10^4 t day^{-1} for both scenarios, as the mouth of the estuary is located 20 km south from the proposed modifications for Ilha do Terrapleno. This value has the same order of magnitude of the export rates estimated by [7], that calculated the value of 3.7×10^4 t day^{-1} and 3.2×10^4 t day^{-1} by [3].

Figure 13. Ilha do Terrapleno. Dark blue (cyan) contour represents the actual (proposed) configuration for the island. White areas indicate the island expansion due to the proposed configuration. Yellow lines indicate the linearized coastline for mooring operations.

The comparison between the actual and proposed scenarios showed changes in the mean depth-averaged current velocity fields both around the island margins and at the adjacent navigation channel (Figure 6). In the proposed scenario, the western portion of the island presented a small increase in mean depth-averaged current velocities (+76%, 0.05 m.s^{-1}), due to the linearization of the island margins (Figure 6C). Likewise, this linearization generated an enlargement of the adjacent navigation channel (central portion), resulting in a decrease in the mean depth-averaged current velocity field (Figures 6C and 8). Except for the extreme northern portion of the channel, where higher mean depth-averaged current velocities were observed, a decrease in the mean depth-averaged current velocity field was observed as a result from the enlargement of this portion of the island, generating a barrier to the flow in the northern portion and a shading region in the northeast region (Figure 6C). Similarly, changes in the mean current velocity profiles along the channel were also observed (Figures 7 and 9).

The current velocity field is directly related to the deposition of suspended sediment at the bottom and one way to present this relationship is through the deposition flux [45], which measures the amount of mass (kg) flowing through an area (m^2) per unit of time (s). This flux is related to the settling velocity (W_c) of the suspended sediment particle and the horizontal components of velocity (u and v). Results for the proposed scenario showed an increase in the deposition flux reaching up to 60% in the southern half of the navigation channel (Figure 10C), which is consistent with the change in the mean depth-averaged current velocities fields observed in Figure 6. Similarly, the deposition flux at the regions adjacent to the island were coherent with the alteration in the mean depth-averaged current velocities. Furthermore, a comparative analysis between scenarios for the bottom evolution in the navigation channel and adjacent region of the island (Figures 11 and 12), were also coherent with the estimated changes in the deposition flux.

Based on these results, it is possible to observe a maximum increase of 40% in the deposition fluxes (which is equivalent to a maximum of 2 cm) during the simulated period (two years), especially in the southern portion of the channel. In the northern portion of the channel, deposition rates ranged from 25% (which is equivalent to a maximum of 1 cm) to −11% (which is equivalent to a maximum of 0.03 cm) towards its northern boundary. Thus, although alterations in mean current velocities, deposition fluxes and bed evolution were observed in a time interval of 2 years, they can be considered small.

Within the critical region (southern portion), the increase of deposition fluxes (40%), results in an increase of 30% (which is equivalent to a maximum of 1 cm) in the thickness of the material deposited at the bottom. Considering the simulation time, the maximum value added for the thickness of the bottom material is still low. Aiming at the cost–benefit of this work, it can be considered viable if this variation in the thickness of the material deposited at the bottom remains close to the quotas projected for the dredging planning, which already take place in the area, without changing its frequency.

A comparative study between scenarios for the Patos Lagoon estuary using the TELEMAC-3D model was previously carried out by [20]. The authors estimated changes in the deposition fluxes in the access channel to the Port of Rio Grande after the expansion work of the two jetties located at the mouth of Patos Lagoon. They concluded that the produced funneling effect at the mouth decreased the local hydrodynamics and increased the deposition of the suspended sediment in the area. However, unfortunately, numerical modeling studies were not carried out before the execution of the jetties modification.

According to [46], the deposition of fine suspended sediment in the navigation channels of the Port of Rio Grande can form layers of high density close to the bottom. In [47], the authors measured the density profile in three sectors (north, central and south) of the same channel presented in this study (between Ilha do Terrapleno and Rio Grande city, Figure 1) and observed layers with density change near the bottom. The values ranged from 1080–1600 kg m^{-3} and the fluid was classified as fluid mud and consolidated mud, respectively [48]. These layers are related to highly concentrated aqueous suspensions of solid material with low density that have a small tendency to consolidation, thus maintaining their mobility [49,50]. Due to its thixotropic properties, the fluid mud presents a non-Newtonian rheological behavior. The SED-3D suspended sediment module, however, is limited to a Newtonian treatment of the bottom, and the simulations were set with a constant value for the critical erosion shear stress. This parametrization does not correspond to the behavior of a non-Newtonian fluid, which presents density stratification varying from fluid mud to slightly consolidated mud, limiting the resuspension estimates when fluid mud is present.

In the study region, only point P1 (Figure 2) and its surroundings reached values equal to or higher for the critical resuspension stress set for the model. However, the analysis of suspended sediment deposition rates for this point and its surroundings, remain valid because the calculated deposition flux is not associated with the occurrence of fluid mud.

Based on the results of this study, the sustainable expansion of the Port of Rio Grande operational capacity considering the creation of 3600 m of berthing wharf areas and minimum environmental impact proved viable when considering the Ilha do Terrapleno proposed configuration (Figure 2). Furthermore, this idea offers the possibility to dispose in land 722,910 m^3 of dredged material, a sustainable alternative to the Port of Rio Grande development, and an inspiration for the sustainable development of other ports worldwide.

6. Conclusions

The present study evaluated changes in the hydrodynamics and suspended sediment transport patterns in the Patos Lagoon estuary based on a proposed scenario for sustainable expansion of the Port of Rio Grande. The study showed that the possibility of disposing dredged material in land to make up for a new configuration for Ilha do Terrapleno may be a good alternative for the Port of Rio Grande, generating a considerable increase in new

berthing wharf areas at the cost of the periodic dredging operations which already take place in the area.

We understand, however, that the inherent limitations of numerical models together with limitations in the input data for this particular study may have underestimated the rates for the deposition of suspended material, mainly around the island. Thus, further attention needs to be addressed to this issue, and field measurements are suggested.

The main lesson learned from this case-study is that sustainable development alternatives are possible but must be extensively investigated prior to any real environmental alteration.

Author Contributions: P.D.d.S.—Conceptualization, methodology, writing—original draft, validation, formal analysis; E.H.F. Conceptualization, methodology, resources, writing-review and editing, visualization, supervision project administration and funding acquisition; G.A.G.—Conceptualization. All authors have read and agreed to the published version of the manuscript.

Funding: This research was sponsored by the Port of Rio Grande Authority (PORTOS RS) and by the LOAD Project (Office of Naval Research, award number N62909-19-1-2145).

Institutional Review Board Statement: Not applicable.

Informed Consent Statement: Not applicable.

Data Availability Statement: The data presented in this study are available on request from the corresponding author.

Conflicts of Interest: The authors declare no conflict of interest.

References

1. Hanson, S.E.; Nicholls, R.J. Demand for Ports to 2050: Climate Policy, Growing Trade and the Impacts of Sea-Level Rise. *Earth's Future* **2020**, *8*, e2020EF001543. [CrossRef]
2. Katsiaras, N.; Simboura, N.; Tsangaris, C.; Hazianestis, I.; Pavlidou, A.; Kapsimalis, V. Impacts dredged-material disposal on the costal soft-bottom marofauna, Saronikos Gulf Greece. *Sci. Environ.* **2015**, *508*, 320–330.
3. Bolam, S.G.; Mcllwaine, P.; Garcia, C. Marine macrofauna traits responses to dredged material disposal. *Mar. Pollut. Bull.* **2021**, *168*, 112412. [CrossRef] [PubMed]
4. Fernandes, E.H.; da Silva, P.D.; Gonçalves, G.A.; Möller, O.O., Jr. Dispersion Plumes in Open Ocean Disposal Sites of Dredged Sediment. *Water* **2021**, *13*, 808. [CrossRef]
5. Alden, R.W.; Young, R.J. Open ocean disposal of materials dredged from a highly industrialized estuary: An evaluation of potential lethal effects. *Arch. Environm. Contam. Toxicol.* **1982**, *11*, 567–576. [CrossRef]
6. Torres, R.J.; Abessa, D.M.S.; Santos, F.C.; Maranho, L.A.; Davanso, M.B.; Nascimento, M.R.L.; Mozeto, A.A. Effects of dredging operations on sediment quality: Contaminant mobilization in dredged sediments from the Port of Santos, SP, Brazil. *J. Soils Sediment* **2009**, *9*, 420–432. [CrossRef]
7. Marques, W.C.; Fernandes, E.H.L.; Moraes, B.C.; Möller, O.O.; Malcherek, A. Dynamics of the Patos Lagoon coastal plume and its contribution to the deposition pattern of the southern Brazilian inner shelf. *J. Geophys. Res. Space Phys.* **2010**, *115*, 1–22. [CrossRef]
8. Krajewski, A.; Sikorska, A.E.; Banasik, K. Modeling suspended sediment concentration in the stormwater outflow from a small detention pond. *J. Environ. Eng.* **2017**, *143*, 1–11. [CrossRef]
9. Santoro, P.; Fossati, M.; Tassi, P.; Huybrechts, N.; Bang, D.P.V.; Piedra-Cueva, J.C.I. A coupled wave-current-sediment transport model for an estuarine system: Application to the Río de la Plata and Montevideo Bay. *Appl. Math. Model.* **2017**, *52*, 107–130. [CrossRef]
10. Tavora, J.; Fernandes, E.H.L.; Thomas, A.C.; Weatherbee, R.; Schettini, C.A.F. The influence of river discharge and wind on Patos Lagoon, Brazil, Suspended Particulate Matter. *Int. J. Remote Sens.* **2019**, *40*, 4506–4525. [CrossRef]
11. Távora, J.; Fernandes, E.H.; Bitencourt, L.P.; Orozco, P.M.S. El Niño Southern Oscillation (ENSO) effects on the vari-ability of Patos Lagoon suspended particulate matter. *Reg. Stud. Mar. Sci.* **2020**, *40*, 101495.
12. Shuklaa, V.K.; Konkaneb, V.D.; Nagendrac, T.; Agrawald, J.D. Dredged Material Dumping Site Selection Using Mathematical Models. *Procedia Eng.* **2015**, *116*, 809–817. [CrossRef]
13. Kim, N.-H.; Pham, V.S.; Hwang, J.H.; Won, N.I.; Ha, H.K.; Im, J.; Kim, Y. Effects of seasonal variations on sediment-plume streaks from dredging operations. *Mar. Pollut. Bull.* **2018**, *129*, 26–34. [CrossRef]
14. Lu, J.; Li, H.; Chen, X.; Liang, D. Numerical Study of Remote Sensed Dredging Impacts on the Suspended Sediment Transport in China's Largest Freshwater Lake. *Water* **2019**, *11*, 2449. [CrossRef]
15. Sharaan, M.; Negm, A. Life Cycle Assessment od Dredged Materials Placement Strategies: Case Study, Damietta Port, Egypt. *Procedia Eng.* **2017**, *181*, 102–108. [CrossRef]
16. Bahgat, M. Optimum use of dredged materials for sustainable shoreline management in Nile Delta. *Water Sci.* **2018**, *32*, 115–128. [CrossRef]

17. Barbosa, M.C.; Almeida, M.D.S.S.D. Dredging and disposal of fine sediments in the state of Rio de Janeiro, Brazil. *J. Hazard. Mater.* **2001**, *85*, 15–38. [CrossRef]
18. Grigalunas, T.; Opaluch, J.J.; Luo, M. The economic costs to fisheries from marine sediment disposal: Case study of Providence, RI, USA. *Ecolog. Econ.* **2001**, *38*, 47–58. [CrossRef]
19. Fries, A.S.; Coimbra, J.P.; Nemazie, D.A.; Summers, R.M.; Azevedo, P.S.; Filoso, S.; Newton, M.; Gelli, G.; Oliveira, R.C.N.; Pessoa, M.A. Guanabara Bay ecosystem helath report card: Science, management and gov-ernance implications. *Reg. Stud. Marice Sci.* **2019**, *25*, 100474.
20. Prumm, M.; Iglesias, G. Impacts of port development on estuarine morphodynamics: Ribadeo (Spain). *Ocean Coast. Manag.* **2016**, *130*, 58–72. [CrossRef]
21. Farhad Sakhaee, F.; Khalili, F. Sediment pattern & rate of bathymetric changes due to construction of breakwater extension at Nowshahr port. *J. Ocean Eng. Sci.* **2021**, *6*, 70–84.
22. Silva, P.D.; Lisboa, P.V.; Fernandes, E.H. Changes on the fine sediment dynamics after the Port of Rio Grande expansion. *Adv. Geosci.* **2015**, *39*, 123–127. [CrossRef]
23. Kjerfve, B. Comparative Oceanography of coast lagoons. *Estuar. Variab.* **1986**, *1*, 63–81.
24. Moller, O.O.; Castaing, P.; Salomon, J.-C.; Lazure, P. The Influence of Local and Non-Local Forcing Effects on the Subtidal Circulation of Patos Lagoon. *Estuaries* **2001**, *24*, 297–311. [CrossRef]
25. Fernandes, E.H.L.; Dyer, K.R.; Moller, O.O. Spatial Gradients in the Flow of Southern Patos Lagoon. *J. Coast. Res.* **2005**, *214*, 759–769. [CrossRef]
26. Calliari, L.J.; Winterwerp, J.C.; Fernandes, E.H.; Cuchiara, D.; Vinzon, S.B.; Sperle, M.; Holland, K.T. Fine grain sediment transport and deposition in the Patos Lagoon–Cassino beach sedimentary system. *Cont. Shelf Res.* **2009**, *29*, 515–529. [CrossRef]
27. Marques, W.C.; Fernandes, E.H.; Monteiro, I.O.; Möller, O.O. Numerical modeling of the Patos Lagoon coastal plume, Brazil. *Cont. Shelf Res.* **2009**, *29*, 556–571. [CrossRef]
28. Herz, R. Circulação das águas de Superfície da Lagoa dos Patos. Ph.D. Thesis, Universidade de São Paulo, São Paulo, Brazil, 1977; 312p.
29. Vaz, A.C.; Möller, O.O.; Almeida, T.L.D. Análise quantitativa da descarga dos rios afluentes da Lagoa dos Patos. *Atlântica* **2006**, *28*, 13–23.
30. Moller, O.O.; Lorenzzentti, J.A.; Stech, J.; Mata, M.M. The Patos Lagoon summertime circulation and dynamics. *Cont. Shelf Res.* **1996**, *16*, 335–351. [CrossRef]
31. Bortolin, E.C.; Távora, J.; Fernandes, E.H.L. Long-Term Variability on Suspended Particulate Matter Loads From the Tributaries of the World's Largest Choked Lagoon. *Front. Mar. Sci.* **2022**, *9*, 836739. [CrossRef]
32. Bitencourt, L.P.; Fernandes, E.H.; Silva, P.D.; Möller, O.O. Spatio-temporal variability of suspended sediment con-centrations in a shallow and turbid laggon. *J. Mar. Syst.* **2020**, *212*, 103454. [CrossRef]
33. Hervouet, J.M. *Hydrodynamics of Free Surface Flows: Modeling with the Finite Element Method*; Wiley: Chichester, UK, 2007.
34. Van Leussen, W. The variability of settling velocities of suspended fine-grained sediment in the Ems estuary. *J. Sea Res.* **1999**, *41*, 109–118. [CrossRef]
35. Partheniades, E. Erosion and Deposition of Cohesive Soils. *J. Hydraul. Div.* **1965**, *91*, 105–139. [CrossRef]
36. Egbert, G.D.; Erofeeva, S.Y. Efficient inverse modeling of barotropic ocean tides. *J. Atmos. Ocean. Technol.* **2002**, *19*, 183–204. [CrossRef]
37. Oliveira, H.A.; Fernandes, E.H.L.; Möller, O.O.; Collares, G.L. Processos Hidrológicos e Hidrodinâmicos da Lagoa Mirim. *Rev. Bras. Recur. Hídricos* **2015**, *20*, 34–45. [CrossRef]
38. Walstra, L.; Van Rijn, L.; Blogg, H.; Van Ormondt, M. Evaluation of a Hydrodynamic Area Model Based on the Coast3d Data at Teignmouth 1999. In Proceedings of the Coastal Dynamics 2001 Conference, Lund D, Lund, Sweden, 11–15 June 2001; pp. D4.1–D4.4.
39. Arnold, J.G.; Moriasi, D.N.; Gassman, P.W.; Abbaspour, K.C.; White, M.J.; Srinivasan, R.; Santhi, C.; Harmel, R.D.; van Griensven, A.; Van Liew, M.W.; et al. SWAT: Model use, calibration, and validation. *Trans. ASABE* **2012**, *55*, 1494–1508. [CrossRef]
40. Fu, B.; Horsburgh, J.S.; Jakeman, A.J.; Gualtieri, C.; Arnold, T.; Marshall, L.; Green, T.R.; Quinn, N.W.T.; Volk, M.; Hunt, R.J.; et al. Modeling Water Quality in Watersheds: From Here to the Next Generation. *Water Resour. Res.* **2020**, *56*, WR027721. [CrossRef] [PubMed]
41. Vargas-Luna, A.; Crosato, A.; Uijttewaal, W.S. Effects of vegetation on flow and sediment transport: Comparative analyses and validation of predicting models. *Earth Surf. Proc. Landf.* **2015**, *40*, 157–176. [CrossRef]
42. Neary, V.S.; Constantinescu, S.G.; Bennett, S.J.; Diplas, P. Effects of Vegetation on Turbulence, Sediment Transport, and Stream Morphology. *Am. Soc. Civ. Eng.* **2012**, *138*, 9. [CrossRef]
43. Marques, W.C.; Fernandes, E.H.; Möller, O.O. Straining and advection contributions to the mixing process of the Patos Lagoon coastal plume, Brazil. *J. Geoflys. Res.* **2010**, *115*, C06019. [CrossRef]
44. Franzen, M.O.; Fernandes, E.H.L.; Siegle, E. Impacts of coastal structures on hydro-morphodynamic patterns and guidelines towards sustainable coastal development: A case studies review. *Reg. Stud. Mar. Sci.* **2021**, *44*, 101800. [CrossRef]
45. Krone, R.B. *Flume Studies of the Transport of Sediment in Estuarine Processes*; Tech. Rep. Hydraulic Engineering Lab., University of California: Berkeley, CA, USA, 1962.

46. Fontoura, J.A.S.; Calliari, L.J. *Diagnóstico do Estudo da Dinâmica Sedimentar e do Comportamento da Linha de Costa no Local de Implantação das Obras do Dique Seco e nas Margens de seu Entorno*; Segundo Relatório; Laboratório de Engenharia Costeira/Laboratório de Oceanografia Geológica: Rio Grande, RS, Brasil, 2007; 23p.
47. Marroig, P.; Vinzon, S. Fluid mud transport from Patos Lagoon to Rio Grande Port, RS, Brazil. In Proceedings of the INTERCOH2015—13th International Conference on Cohesive Sediment Transport Processes, Leuven, Belgium, 7–11 September 2015.
48. Mehta, A.J.; Samsami, F.; Khare, Y.P. Fluid Mud Properties in Nautical Depth Estimation. *J. Waterw. Port Coast. Ocean. Eng.* **2014**, *140*, 210–222. [CrossRef]
49. Mcanally, W.H.; Friedrichs, C.; Hamilton, D. Management of Fluid Mud in Estuaries, Bays, and Lakes. I: Present State of Understanding on Character and Behavior. *J. Hydraul. Eng.* **2007**, *133*, 23–38. [CrossRef]
50. Wurpts, R. 15 Years Experience with Fluid Mud: Definition of the Nautical Bottom with Rheological Parameters. *Terra e Aqua* **2005**, *99*, 22–32.